

---

# SCALAR REPRESENTATION OF 2D STEADY VECTOR FIELDS

---

 **Holger Theisel**

Department of Computer Science  
University of Magdeburg  
Magdeburg, Germany  
theisel@ovgu.de

 **Michael Motejat**

Department of Computer Science  
University of Magdeburg  
Magdeburg, Germany  
michael@isg.cs.uni-magdeburg.de

 **Janos Zimmermann**

Department of Computer Science  
University of Magdeburg  
Magdeburg, Germany  
janos@isg.cs.uni-magdeburg.de

 **Christian Rössl**

Department of Computer Science  
University of Magdeburg  
Magdeburg, Germany  
roessler@isg.cs.uni-magdeburg.de

January 15, 2024

## ABSTRACT

We introduce a representation of a 2D steady vector field  $\mathbf{v}$  by two scalar fields  $a$ ,  $b$ , such that the isolines of  $a$  correspond to stream lines of  $\mathbf{v}$ , and  $b$  increases with constant speed under integration of  $\mathbf{v}$ . This way, we get a direct encoding of stream lines, i.e., a numerical integration of  $\mathbf{v}$  can be replaced by a local isoline extraction of  $a$ . To guarantee a solution in every case, gradient-preserving cuts are introduced such that the scalar fields are allowed to be discontinuous in the values but continuous in the gradient. Along with a piecewise linear discretization and a proper placement of the cuts, the fields  $a$  and  $b$  can be computed. We show several evaluations on non-trivial vector fields.

**Keywords** Visualization · scalar fields · vector fields

## 1 Introduction

Scalar fields and vector fields are perhaps the most common data classes in (Scientific) Visualization. For both classes, a huge amount of visualization techniques has been developed over the last decades. Vector fields are usually the more complicated data class because firstly they contain more data per point in the domain and secondly transportation issues of particles are involved. Because of this, scalar field visualization is much further developed than vector field visualization.

A general approach to vector field visualization is to derive one (ore more) scalar fields from a vector field, and then apply scalar field visualization on them. While many scalar fields have been proposed to visualize vector fields (like vector magnitude, divergence, FTLE,...), all of them come with a loss of information. In particular, they do not encode the transport of particles, i.e., the location of particles after a certain integration time cannot be computed (neither directly nor indirectly by numerical integration) from these scalar fields.

Flow visualization has a variety of goals and applications, ranging from understanding of fundamental flow phenomena to the analysis of concrete simulations or measurements. We identify generic problems that frequently occur in various applications of flow visualization:

- *The integration problem:* many algorithms in vector field visualization are based on the numerical integration of stream lines / particle trajectories. While stream line integration is numerically well-understood, it is still source of error because of error accumulation during the integration. Error accumulation is an issue for every numerical stream lines integration technique, no matter how involved it is.

- *The connectivity problem*: many algorithms rely on an efficient approach to answer the following question: given two points  $\mathbf{x}_1, \mathbf{x}_2$ , does a streamline starting from  $\mathbf{x}_1$  hit the point  $\mathbf{x}_2$ ? If not, on which side (in 2D) and at which distance the line passes by?

These two problems are generic: they appear in many visualization techniques. Having efficient solutions for them would affect different existing visualization techniques.

In this paper, we follow the established path of finding scalar fields representing vector fields. However, our new approach is to find scalar fields that solve both the integration problem and the connectivity problem. In other words: we search for derived scalar fields such that both integration and connectivity can be solved by a local lookup, a procedure much faster and less error prone than numerical stream line integration. In particular, we want to find a scalar field such that the stream lines of the vector field correspond to isolines of the scalar field.

Unfortunately, in general a scalar field with isolines following stream lines of vector fields does not exist. To overcome this, we weaken our goal by allowing gradient-preserving cuts and a special treatment of critical points. With this, we find scalar representations of vector fields that directly encode particle transportation. We apply our approach to introduce a strictly local (i.e., without any numerical integration) image based flow visualization technique.

## Notation

We consider a 2D steady vector field  $\mathbf{v}(\mathbf{x})$  over a simple connected limited domain  $D \subset \mathbb{R}^2$  with disk topology where  $\delta D$  is the boundary curve of  $D$ . We assume that  $\delta D$  is given as a closed differentiable parametric curve  $\mathbf{d}(s)$ . Let  $\phi(\mathbf{x}, \tau)$  denote the flow map of  $\mathbf{v}$ , i.e.,  $\phi(\mathbf{x}, \tau)$  is the location to be landed by integrating  $\mathbf{v}$  starting from  $\mathbf{x}$  over an integration time  $\tau$ . Let  $\mathbf{J}$  be the Jacobian matrix of  $\mathbf{v}$ , and let

$$\bar{\mathbf{v}}(\mathbf{x}) = \frac{\mathbf{v}}{\|\mathbf{v}\|}, \quad \bar{\mathbf{w}}(\mathbf{x}) = \begin{pmatrix} 0 & -1 \\ 1 & 0 \end{pmatrix} \cdot \bar{\mathbf{v}}$$

be the normalized and normalized perpendicular field of  $\mathbf{v}$ . Further,  $\nabla a$  denotes the gradient of a scalar field  $a$ , while  $\nabla_{\perp} a = \begin{pmatrix} 0 & -1 \\ 1 & 0 \end{pmatrix} \nabla a$  denotes its co-gradient.

## 2 Problem description and analysis

Given a 2D steady vector field  $\mathbf{v}(\mathbf{x})$ , we search for two smooth and differentiable scalar fields  $a(\mathbf{x}), b(\mathbf{x})$  with the following properties:

$$\nabla a \neq \mathbf{0} \tag{1}$$

$$\mathbf{v}^T \nabla a = 0 \tag{2}$$

$$\mathbf{v}^T \nabla b = 1 \tag{3}$$

for all  $\mathbf{x} \in D$ . (1) and (2) make sure that a stream line of  $\mathbf{v}$  is an isoline of  $a$ . (3) makes sure that  $b$  increases with unit speed under integrating a stream line. This way, stream line integration in  $\mathbf{v}$  reduces to isocurve intersection of  $a$  and  $b$  by

$$a(\phi(\mathbf{x}, \tau)) = a(\mathbf{x}), \quad b(\phi(\mathbf{x}, \tau)) = b(\mathbf{x}) + \tau. \tag{4}$$

Unfortunately, a field  $a$  fulfilling (1), (2) does in general not exist. The simplest counterexample is the linear field  $\mathbf{v}(\mathbf{x}) = (x, y)^T$  for which no smooth field  $a$  can exist. In general, if  $\mathbf{v}$  is divergence-free, a field  $a$  exists: the stream function. Also for the field  $b$ , existence is not ensured: for divergence-free  $\mathbf{v}$ , a contradiction in  $b$  is created on a closed stream line after one turn.

In order to cope with the problem, we allow a certain weakening of the conditions for  $a, b$  that allow a unique solution but still allow to solve the integration and connectivity problem by an isovalue lookup. In particular, we introduce two concepts: gradient preserving cuts and a special treatment of areas around critical points.

## 3 Related work

We divide the review of existing work in four parts: vector field visualization, scalar field visualization, scalar field representation of vector fields, and finding optimal cuts in shape processing.

**Vector field visualization** Vector field visualization is one of the core topics in Scientific Visualization. While in many cases the vector data describe flow phenomena, other effects represented by vector field data exist as well, such as dynamical systems or magnetic fields. A variety of techniques for vector field visualization has been developed, ranging from texture based techniques Laramée et al. [2004] over feature extraction Post et al. [2003], Günther and Theisel [2017], topological methods Pobitzer et al. [2011a], Salzbrunn et al. [2008] until illustrative techniques Brambilla et al. [2012]. Most relevant for our work are topological techniques because they develop a partition of the vector fields in to critical points and separatrices of of relevance for the new approaches.

Topological methods for 2D vector fields have been introduced to the visualization community in Helman and Hesselink [1989]. Later they were extended to higher order critical points Scheuermann et al. [1998], boundary switch points de Leeuw and van Liere [1999a], and closed separatrices Wischgoll and Scheuermann [2001]. In addition, topological methods have been applied to simplify de Leeuw and van Liere [1999a,b], Tricoche et al. [2000, 2001], smooth Westermann et al. [2001], compress Lodha et al. [2000], Suresh Lodha and Renteria [2003], Theisel et al. [2003a] and construct Theisel [2002], Weinkauff et al. [2004a] vector fields. 3D topological feature are considered in Globus et al. [1991], Helman and Hesselink [1991], Mahrous et al. [2003, 2004], Theisel et al. [2003b], Weinkauff et al. [2004b]. State-of-the-Art-Reports on topological methods for flow visualization can be found in Laramée et al. [2007], Pobitzer et al. [2011b], Wang et al. [2016], Heine et al. [2016].

Topological methods can be applied only to steady vector fields because they require integration over an infinitely long integration time. For unsteady fields, Lagrangian Coherent Structures (LCS) have been established to find regions of homogeneous flow behavior. One of the most prominent approaches for this is the computation of ridge structures in FTLE fields, as introduced by Haller Haller [2001], Haller and Yuan [2000]. To consider spatial separation only, Pobitzer et al. [2012] weighted FTLE values by their angle to the separation direction. FTLE ridges were proposed for a variety of applications Haller [2002], Lekien et al. [2005], Shadden et al. [2009], Weldon et al. [2008]. Shadden et al. [2005] showed that ridges of FTLE are approximate material structures, i.e., they converge to material structures for increasing integration times. This fact was used in Sadlo and Weiskopf [2010], Uffinger et al. [2013] to extract topological structures and in Lipinski and Mohseni [2010] to accelerate the FTLE computation in 2D flows. Also in the visualization community, different approaches have been proposed to increase performance, accuracy and usefulness of FTLE as a visualization tool Günther et al. [2016], Garth et al. [2009, 2007], Sadlo and Peikert [2009, 2007], Sadlo et al. [2011].

In recent years approaches have evolved that aim at finding suitable moving frames of the underlying coordinate system to study the flow Bhatia et al. [2014], Wiebel et al. [2007] or develop Galilean invariant detectors directly Bujack et al. [2016]. This way, finite-time studies of time-dependent fields is lead back to a topological analysis of a derived steady field.

We also note that discrete versions of vector field topology have been developed based on either Forman's discrete Morse theory Forman [2001], Reininghaus and Hotz [2011] or Morse decomposition Mischaikow et al. [2007]. Other approaches use edge maps Bhatia et al. [2012] or robustness considerations for critical points treatment Skraba et al. [2016], Wang et al. [2013].

**Scalar field visualization** Scalar fields are another well-researched standard data class in Scientific Visualization. A variety of techniques has been developed for scalar fields, ranging from isosurface extraction over direct volume rendering to feature extraction. In particular, topological features have been proven successful. We mention Morse-Smale complexes and the Reeb graph.

The Morse-Smale complex is a topological structure representing the gradient-flow behavior of a scalar field. Of particular interest for visualization are combinatorial approaches based on piecewise linear scalar fields as introduced in Edelsbrunner et al. [2001] and later extended in several ways Bremer et al. [2004], Edelsbrunner et al. [2003], Gyulassy et al. [2005], Lewiner et al. [2004], Gyulassy et al. [2015, 2007]. The combinatorial approach makes the extraction of Morse-Smale complexes relevant because it allows effective algorithms with guarantees about their correctness.

The Reeb graph considers components of contours and their topological changes. They have been applied to control the removal of topological features Cignoni et al. [2000], Carr et al. [2004], Guskov and Wood [2001], Takahashi et al. [2004], Carr et al. [2003], Tierny et al. [2012].

**Vector field approximation by scalar fields** Scalar fields are simpler structures than vector fields. So, it is not surprising that research came up with approaches to represent vector fields (in particular flow fields and vorticity fields) as scalar fields. The Clebsch map Clebsch [1859] represents divergence-free velocity and vorticity fields as a certain combination of gradients of scalar fields. Such representations have been used to visualize Kotiuga [1991], analyze Jeong and Hussain [1995] and simplify flows Brandenburg [2010], He and Yang [2016,?]. Unfortunately, such representations cannot be exact in the general case Graham and Henyey [2000], resulting in either approximate

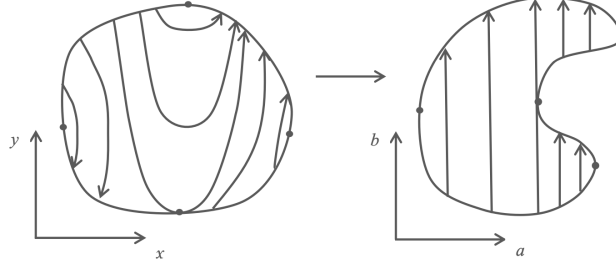


Figure 1: Finding the fields  $a, b$  can be interpreted as searching for a domain transformation of  $\mathbf{v}$  to  $(0, 1)^T$ .

representations Chern et al. [2017] or applications restricting to certain subclasses of divergence-free vector fields Angelidis and Singh [2007], von Funck et al. [2006].

**Optimal cuts on shapes** Many algorithms in Geometry processing require open surfaces with well-defined boundaries, such as surface parametrization Zigelman et al. [2002], Hormann et al. [2008] or quad-remeshing Ebke et al. [2016], Campen and Kobbelt [2014]. For closed input surfaces, cutting algorithms are necessary. Since the placement of the cuts influences the result of the algorithms, "optimal" cuts are searched. Several criteria for optimality have been proposed and applied Erickson and Har-Peled [2002].

## 4 Solution on simple vector fields

In this section, we provide a solution for  $a, b$  for simple vector fields.

**Definition 1** A vector field  $\mathbf{v}$  to be simple if it fulfills the following property: for every  $\mathbf{x} \in D$  we reach the boundary after a finite integration time both in forward and backward integration.

From this it follows that  $\mathbf{v}$  has neither critical points nor closed orbits.

For simple vector fields, the search for  $a, b$  can be interpreted as a domain transformation of  $\mathbf{v}$  in the domain  $D$  to the constant vector field  $(0, 1)^T$  in the new domain  $D'$ . Figure 1 gives an illustration. Note that (1)–(3) does not give unique solutions for  $a, b$ . Among all solutions for  $a, b$ , we search for the ones the with

$$\int_D (\|\nabla a\| - \|\mathbf{v}\|)^2 d\mathbf{x} \rightarrow \min \quad (5)$$

$$\int_D \|\nabla b\|^2 d\mathbf{x} \rightarrow \min. \quad (6)$$

Given a point  $\mathbf{x} \in D$ , let  $\tau_0(\mathbf{x}), \tau_1(\mathbf{x})$  be the integration time to reach the boundary of  $D$  starting from  $\mathbf{x}$  in backward and forward direction respectively, i.e.:

$$\tau_0(\mathbf{x}) \leq 0 \leq \tau_1(\mathbf{x}) \quad (7)$$

$$\phi(\mathbf{x}, \tau_0(\mathbf{x})), \phi(\mathbf{x}, \tau_1(\mathbf{x})) \in \delta D \quad (8)$$

$$\phi(\mathbf{x}, \tau) \notin \delta D \text{ for } \tau \in ]\tau_0(\mathbf{x}), \tau_1(\mathbf{x})[. \quad (9)$$

Further, we define the end points of the integration from  $\mathbf{x}$  as  $\mathbf{d}_0(\mathbf{x}) = \phi(\mathbf{x}, \tau_0(\mathbf{x}))$  and  $\mathbf{d}_1(\mathbf{x}) = \phi(\mathbf{x}, \tau_1(\mathbf{x}))$ . Also, we define the boundary points in terms of the parametrization  $s$  for the boundary curve  $s(s)$ :  $s_0(\mathbf{x}), s_1(\mathbf{x})$  are defined by

$$\mathbf{d}(s_0(\mathbf{x})) = \mathbf{d}_0(\mathbf{x}) \quad , \quad \mathbf{d}(s_1(\mathbf{x})) = \mathbf{d}_1(\mathbf{x}). \quad (10)$$

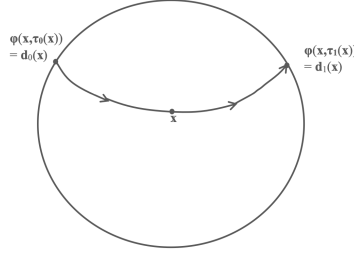
Figure 2 gives an illustration. Since  $\mathbf{v}$  is simple, there is a unique  $\tau_0, \tau_1, \mathbf{d}_0, \mathbf{d}_1, s_0, s_1$  for every  $\mathbf{x} \in D$ . Also, (4) gives that it is sufficient to compute  $a, b$ , on the boundary of  $D$  only by

$$a(\mathbf{x}) = a(\mathbf{d}_0(\mathbf{x})) = a(\mathbf{d}_1(\mathbf{x})) \quad (11)$$

$$b(\mathbf{x}) = b(\mathbf{d}_0(\mathbf{x})) - \tau_0(\mathbf{x}) = b(\mathbf{d}_1(\mathbf{x})) - \tau_1(\mathbf{x}) \quad (12)$$

### 4.1 Computing $a, b$

The computation of both  $a$  and  $b$  is done in the following steps:


 Figure 2: Definition of  $\tau_0(\mathbf{x})$ ,  $\tau_1(\mathbf{x})$ ,  $\mathbf{d}_0(\mathbf{x})$ ,  $\mathbf{d}_1(\mathbf{x})$ .

1. Compute  $a_s(s) = \frac{d a(\mathbf{d}(s))}{d s}$ , and  $b_s(s) = \frac{d b(\mathbf{d}(s))}{d s}$ , i.e., the derivatives of  $a, b$  along the boundary curve.
2. Compute  $a(s) = a(\mathbf{d}(s))$ ,  $b(s) = b(\mathbf{d}(s))$  by integrating  $a_s(s), b_s(s)$ , respectively.
3. Compute  $a(\mathbf{x}), b(\mathbf{x})$  in the inner domain by applying (11), (12).

### Computing $a$

For  $\mathbf{x} \in D$ , we compute the separating function Friederici et al. [2017] along the stream as

$$s_l(\mathbf{x}, \tau) = \int_{\tau_0(\mathbf{x})}^{\tau} \bar{\mathbf{w}}(\phi)^T \mathbf{J}(\phi) \bar{\mathbf{w}}(\phi) d\tau \quad (13)$$

with  $\phi = \phi(\mathbf{x}, t)$  that describes the behavior of "adjacent" isolines in  $a$ . We search for the scalar  $s_m(\mathbf{x})$  minimizing

$$\int_{\tau_0(\mathbf{x})}^{\tau_1(\mathbf{x})} \left( e^{-s_l(\mathbf{x}, \tau) - s_m(\mathbf{x})} - \|\mathbf{v}(\phi(\mathbf{x}, \tau))\| \right)^2 d\tau \rightarrow \min. \quad (14)$$

Fortunately, this has a closed form solution for  $s_m(\mathbf{x})$ :

$$s_m(\mathbf{x}) = \ln \left( \frac{\int_{\tau_0(\mathbf{x})}^{\tau_1(\mathbf{x})} (e^{-s_l(\mathbf{x}, \tau)})^2 d\tau}{\int_{\tau_0(\mathbf{x})}^{\tau_1(\mathbf{x})} \|\mathbf{v}(\phi(\mathbf{x}, \tau))\| e^{-s_l(\mathbf{x}, \tau)} d\tau} \right). \quad (15)$$

Finally, we compute

$$s(\mathbf{x}) = s_l(\mathbf{x}, 0) + s_m(\mathbf{x}). \quad (16)$$

The field  $s(\mathbf{x})$  steers the gradient of  $a$  by

$$\nabla a = e^{-s} \bar{\mathbf{w}}. \quad (17)$$

### Computing $b$

If  $b$  is set on a stream line, we need to set it on the "adjacent" stream line as well. In other words, we need to study and optimize the behavior of  $\nabla b$ . It turns out that – similar to  $a$  – we have one degree of freedom to steer  $\nabla b$  along the stream line. In the best case we would have  $(\nabla a)^T \nabla b = 0$ . However, if we set this property in  $\mathbf{x}$ , it does not advect along the stream line.

At a point  $\mathbf{x}$ , we consider a point  $\mathbf{y}$  in its neighborhood and observe  $\mathbf{y} - \mathbf{x}$  under the local (changing) coordinate system  $(\bar{\mathbf{v}}, \bar{\mathbf{w}})$ :

$$p = \bar{\mathbf{v}}^T (\mathbf{y} - \mathbf{x}), \quad q = \bar{\mathbf{w}}^T (\mathbf{y} - \mathbf{x}), \quad r = \frac{p}{q} = \tan \alpha. \quad (18)$$

Figure 3 gives an illustration of the setup.

We assume that  $(\mathbf{y} - \mathbf{x})$  is the direction of the co-gradient of  $b$ . We observe how,  $p, q, r$  behave over stream line integration:

$$\frac{dp}{d\tau} = \bar{\mathbf{v}}^T \mathbf{J} \bar{\mathbf{v}} p + (\bar{\mathbf{v}}^T \mathbf{J} \bar{\mathbf{w}} + \bar{\mathbf{w}}^T \mathbf{J} \bar{\mathbf{v}}) q \quad (19)$$

$$\frac{dq}{d\tau} = \bar{\mathbf{w}}^T \mathbf{J} \bar{\mathbf{w}} q \quad (20)$$

$$\frac{dr}{d\tau} = (\bar{\mathbf{v}}^T \mathbf{J} \bar{\mathbf{v}} - \bar{\mathbf{w}}^T \mathbf{J} \bar{\mathbf{w}}) r + (\bar{\mathbf{v}}^T \mathbf{J} \bar{\mathbf{w}} + \bar{\mathbf{w}}^T \mathbf{J} \bar{\mathbf{v}}). \quad (21)$$

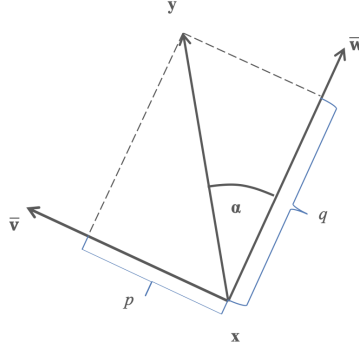


Figure 3: setup of local moving coordinate system.

With (21) we can compute the optimal  $r$  along a stream line by

$$\int_{\tau_0(\mathbf{x})}^{\tau_1(\mathbf{x})} (r(\phi(\mathbf{x}, \tau)))^2 d\tau \rightarrow \min. \quad (22)$$

This should be linear in  $r$ . Note again that  $r$  defines the direction of the co-gradient of  $b$ . Together with (3),  $\nabla b$  is uniquely defined.

## 5 Gradient-preserving cuts

Keep in mind that the approach to compute  $a$  and  $b$  in section 4 works only on simple vector fields. To make it applicable to every vector field, we introduce gradient-preserving cuts.

In the following we give a definition of gradient-preserving cuts of a 2D scalar field along a cutting curve  $\mathbf{c}(t)$ :

**Definition 2** Given is a 2D scalar field  $s(x, y)$  and a regularly parametrized curve  $\mathbf{c}(t)$  in the domain of  $s$ . We assume  $s$  to be at least  $C^1$  continuous outside  $\mathbf{c}$ . The field  $s$  has a gradient-preserving cut along  $\mathbf{c}$  if

1.  $s$  is undefined on  $\mathbf{c}$ .
2.  $\lim_{\mathbf{x} \rightarrow \mathbf{c}(t), \text{left}} s(\mathbf{x}) - \lim_{\mathbf{x} \rightarrow \mathbf{c}(t), \text{right}} s(\mathbf{x}) = h$
3.  $\lim_{\mathbf{x} \rightarrow \mathbf{c}(t), \text{left}} \nabla s(\mathbf{x}) = \lim_{\mathbf{x} \rightarrow \mathbf{c}(t), \text{right}} \nabla s(\mathbf{x})$

where  $\lim_{\mathbf{x} \rightarrow \mathbf{c}(t), \text{left}}$  considers all points  $\mathbf{x}$  being "left" of the curve, i.e.,  $\det(\dot{\mathbf{c}}(t), (\mathbf{x} - \mathbf{c}(t))) > 0$  and  $\dot{\mathbf{c}}$  is the tangent vector of  $\mathbf{c}$ . Further,  $h$  is a non-zero constant.

Definition 2 states that along  $\mathbf{c}(t)$ ,  $s$  has a well-defined discontinuity but nevertheless a continuous gradient. Figure 4 shows an example of a gradient-preserving cut of a 1D function  $s(x)$ . Figure 5 shows a 2D gradient-preserving cut

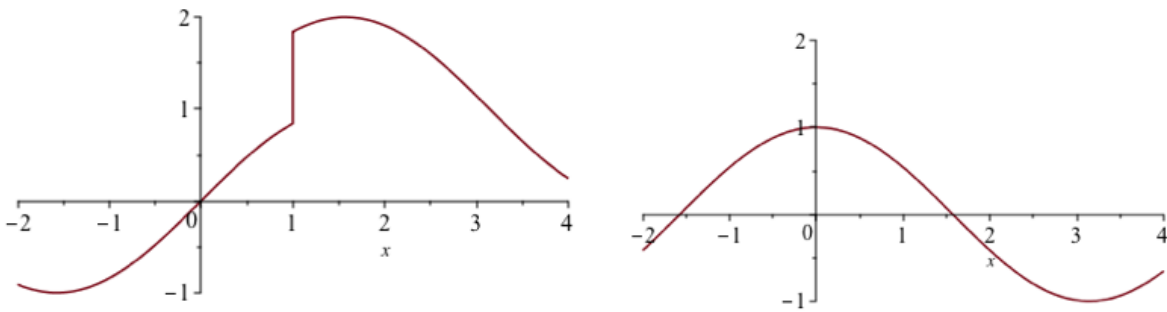


Figure 4: left: 1D field with gradient-preserving cut; right: its derivative.

in a scalar field as height field along with isolines. Note that the isolines appear continuously even though the field has a cut. Since scalar fields with gradient-preserving cuts are gradient continuous, they have continuous gradient

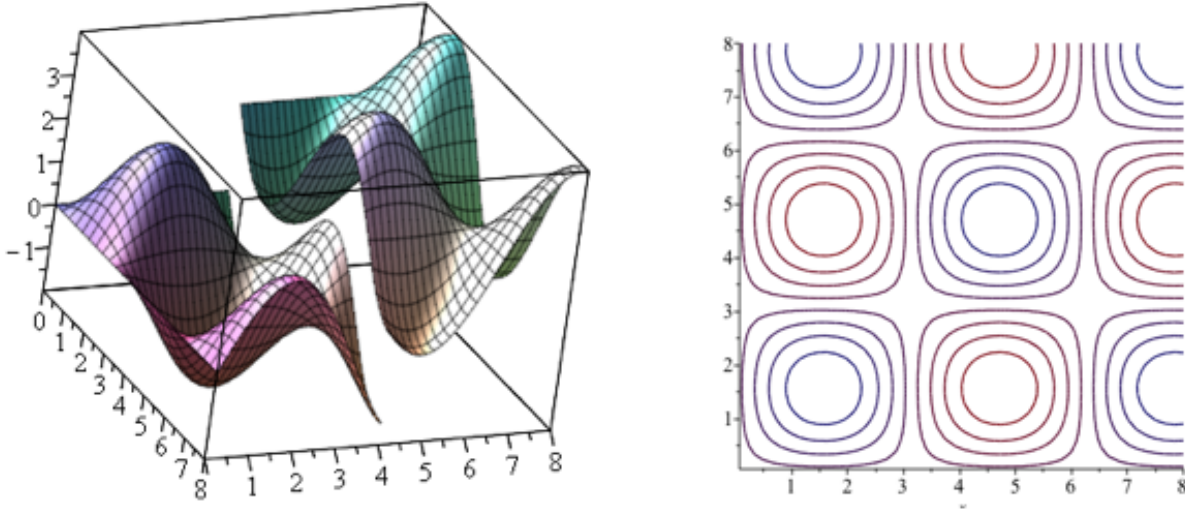


Figure 5: left: 2D field with gradient-preserving cut as height field; right: isocontours

and co-gradient fields. Hence, the potential advances still hold under slight modifications of the algorithms: for isocontouring approaches to integrate a co-gradient field, the consideration of an offset  $h$  of isovalues across the cutting curve is necessary. For an integration of a gradient ascent/descent, a special treatment across the cutting curve is necessary.

## 6 Treatment of critical points

Consider the 2D linear vector field  $\mathbf{v}(\mathbf{x}) = \mathbf{J} \mathbf{x}$  which has a critical point at the origin. Depending on an eigenanalysis of the Jacobian  $\mathbf{J}$ , we discuss the following cases (let  $\lambda_1, \lambda_2$  be the eigenvalues of  $\mathbf{J}$  and  $\mathbf{r}_1, \mathbf{r}_2$  the corresponding eigenvectors):

*Case 1:*  $\mathbf{v}$  has a saddle, i.e.,  $\lambda_1 < 0 < \lambda_2$ . In this case it is a straightforward exercise in algebra to that the scalar field

$$s(\mathbf{x}) = \det(\mathbf{x}, \mathbf{r}_1)^{-\lambda_1} \det(\mathbf{x}, \mathbf{r}_2)^{\lambda_2} \quad (23)$$

with  $p^q = \text{sign}(p) \|p\|^q$  fulfills 2., i.e.,  $\mathbf{v}^T \nabla s = 0$ . Note that (23) does not even need a gradient-preserving cut to fulfill 2. Figure 6 illustrates this for the example field  $\mathbf{v}_1 = \begin{pmatrix} -2 & \frac{3}{2} \\ 0 & 1 \end{pmatrix} \mathbf{x}$  by showing the LIC image of  $\mathbf{v}$  (left),  $s$  as height field (middle), and isocontours of  $s$  (right).

*Case 2:*  $\mathbf{v}$  has a source or a sink with real eigenvalues of  $\mathbf{v}$ , i.e.,  $\lambda_1 \leq \lambda_2 < 0$  or  $0 < \lambda_1 \leq \lambda_2$ . In this case the scalar field

$$s(\mathbf{x}) = \arctan(\det(\mathbf{x}, \mathbf{r}_1)^{-\lambda_1} \det(\mathbf{x}, \mathbf{r}_2)^{\lambda_2}) \quad (24)$$

fulfills 2. Moreover, here we have a gradient-preserving cut starting from the origin that is due to the arctan function. Figure 7 illustrates this for the vector field  $\mathbf{v}_2 = \begin{pmatrix} 2 & -\frac{1}{2} \\ 0 & 1 \end{pmatrix} \mathbf{x}$ .

*Case 3:*  $\mathbf{v}$  is a source or a sink with imaginary eigenvalues of  $\mathbf{J}$ , i.e., a swirling behavior around the critical point. In this case, the scalar field

$$s(\mathbf{x}) = \alpha \arctan\left(\frac{\mathbf{a}^T \mathbf{x}}{\beta \mathbf{b}^T \mathbf{x}}\right) + \beta \ln(\mathbf{x}^T \mathbf{C} \mathbf{x}) \quad (25)$$

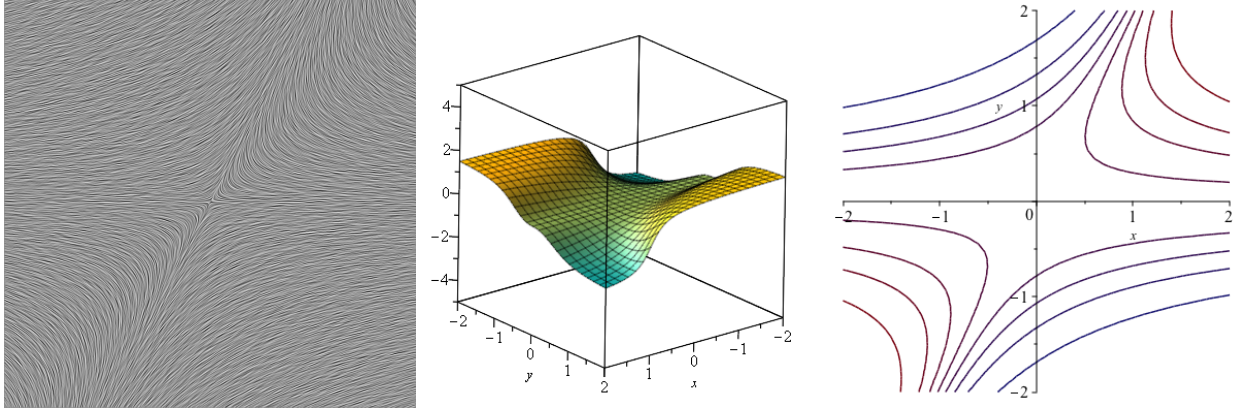


Figure 6: Linear vector field  $\mathbf{v}_1$  containing a saddle; LIC image of  $\mathbf{v}_1$  (left),  $s$  as height field (middle), isocontours of  $s$  (right).

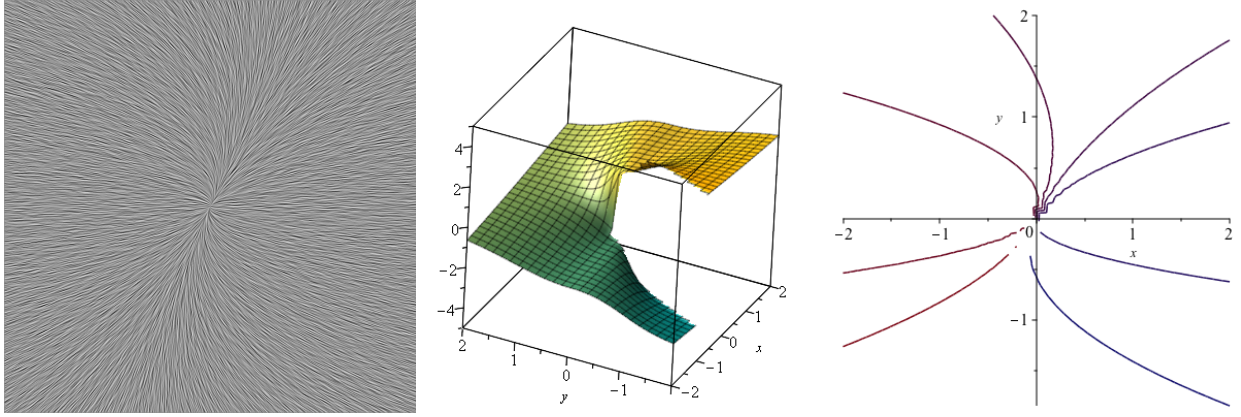


Figure 7: Linear vector field  $\mathbf{v}_2$  with two positive real eigenvalues of  $\mathbf{J}$ ; LIC image of  $\mathbf{v}_2$  (left),  $s$  as height field (middle), isocontours of  $s$  (right).

with

$$\mathbf{R} = \begin{pmatrix} 0 & -1 \\ 1 & 0 \end{pmatrix}, \quad \hat{\mathbf{J}} = \frac{1}{2} (\mathbf{R}\mathbf{J} + (\mathbf{R}\mathbf{J})^T), \quad \alpha = \text{Trace}(\mathbf{J})$$

$$\beta = \sqrt{\|\det \hat{\mathbf{J}}\|}, \quad \mathbf{a}^T = (1, 0) \hat{\mathbf{J}}, \quad \mathbf{b}^T = (1, 0) \mathbf{R}, \quad \mathbf{C} = \hat{\mathbf{J}}.$$

Figure 8 illustrates this for the field  $\mathbf{v}_3 = \begin{pmatrix} 1 & 4 \\ -2 & 3 \end{pmatrix} \mathbf{x}$ .

Based on these cases, we formulate the following:

**Corollary 1** *Every 2D linear vector field can be described as co-gradient field of a scalar field  $a$  with a gradient-preserving cut.*

## 7 Placement of the cuts

Cuts must be placed such that all critical points are covered and the vector field  $\mathbf{v}$  is divided into a set of simple vector fields. To this end, we set the cuts manually by defining a polygon connecting all critical points and to connect to one additional point at the boundary of the domain. A similar approach for defining cuts has been applied in Theisel et al. [2004] to compute isolated closed stream lines.



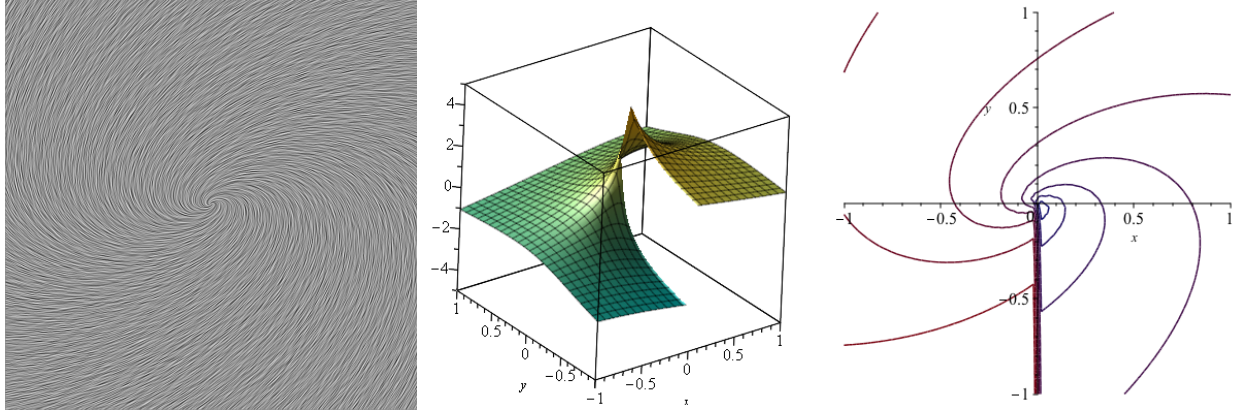


Figure 8: Vector field  $\mathbf{v}_3$  with imaginary eigenvalues of the Jacobian; LIC image of (left),  $s$  as height field (middle), isocontours of  $s$  (right).

## 8 Discretization and solution

We assume a piecewise linear vector field over a triangulation of the domain  $D$ . We search for piecewise scalar fields  $a, b$  over the same triangulation, i.e., the unknown scalar values  $a, b$  at the vertices of the triangulation. The general algorithm is as follows:

1. Set the cuts in the domain  $D$ .
2. Compute  $a, b$  along the boundary of  $D$ , i.e.,

$$a(s) = a(\mathbf{d}(s)) \quad , \quad b(s) = b(\mathbf{d}(b)). \quad (26)$$

3. For every inner point  $\mathbf{x}$  on the triangulation, compute  $a(\mathbf{x})$  and  $b(\mathbf{x})$  by applying (11), (12).

More information is necessary for step 2. We compute all boundary switch points Weinkauff et al. [2004c] on the boundary of  $D$  that divide the boundary in alternating areas of inflow and outflow, respectively. We consider outflow areas only and compute  $a, b$  by applying (13)–(22). For inflow areas, the corresponding values  $a, b$  are computed by applying (11), (12), respectively.

## 9 Results

We apply our approach to a number of test fields. Figure 9 shows a piecewise linear vector field with 3 swirling sources and a saddle. Figure 9(right) shows a LIC image of the field as well as the cuts. Figure 9(left) shows the computed piecewise linear field  $a$  as height field. Also the underlying triangulation for the piecewise linear fields are shown. The projected lines in figure 9(left) show isolines of  $a$  that correspond to stream lines of  $\mathbf{v}$ . Note that we can see a clear discontinuity of  $a$  at the cuts, but no discontinuities are visible in the isolines, which is due to the gradient-preservation property.

Figure 10 shows the approach for a vector field with 2 sources, 2 sinks and 2 saddles.

## 10 Conclusion

We presented a principal solution to represent 2D vector fields as scalar fields. Further research is necessary concerning the comparison of accuracy of isoline extraction of  $a$  vs. a standard numerical stream line integration of  $\mathbf{v}$ . Also, further and more complex data sets need to be evaluated.

An extension to 2D time-dependent as well as to 3D vector fields is non-trivial, but there is no fundamental reason that prevents the extension. We leave this extension to future research.

## Acknowledgements

This work was partially supported by DFG grant TH 692/17-1.

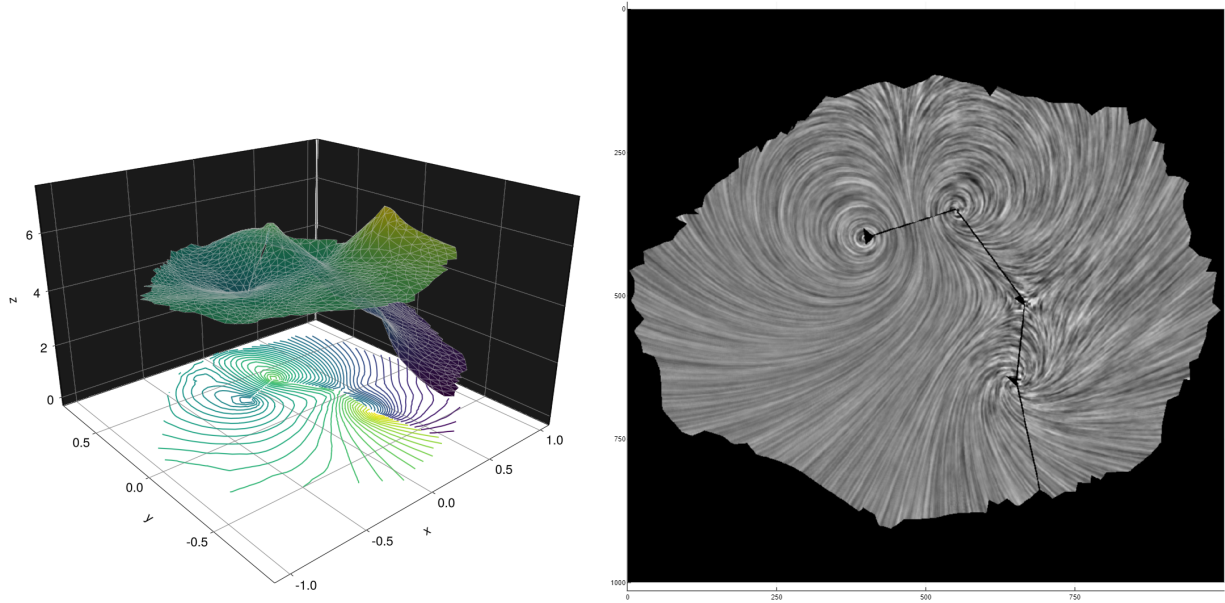


Figure 9: Vector field with 3 swirling sources and a saddle; 3d image of the constructed scalar field (left), LIC of the vector field (right).

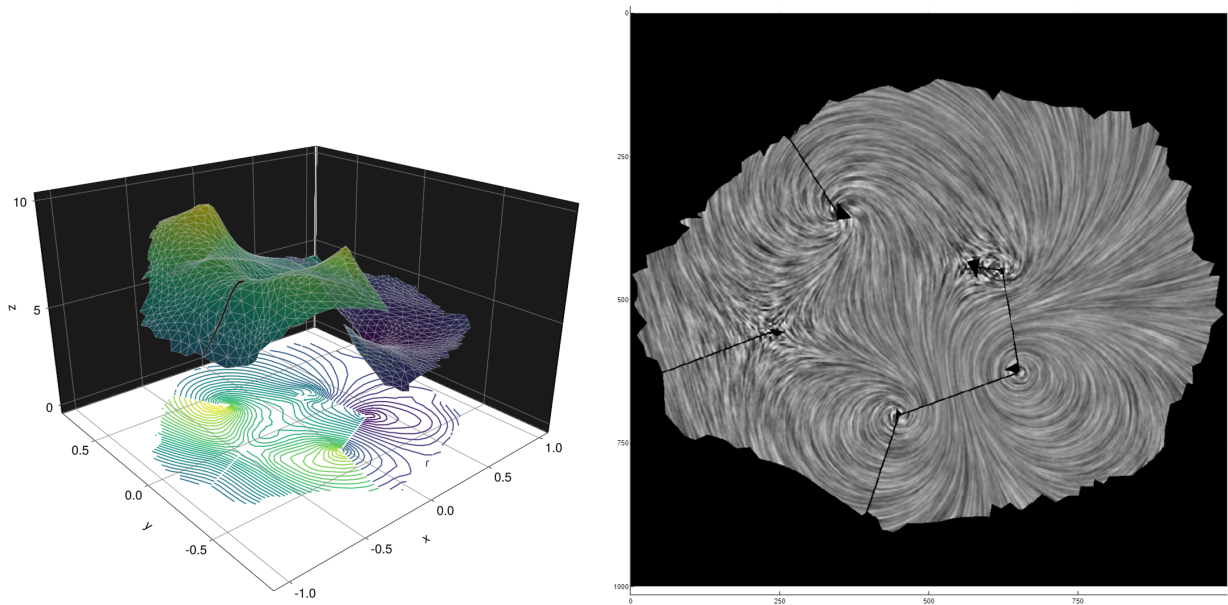


Figure 10: Vector field with 2 sources, 2 sinks and 2 saddles; 3d image of the constructed scalar field (left), LIC of the vector field (right).

## References

- Robert S. Laramee, Helwig Hauser, Helmut Doleisch, Benjamin Vrolijk, Frits H. Post, and Daniel Weiskopf. The state of the art in flow visualization: Dense and texture-based techniques. *Computer Graphics Forum*, 23(2):203–221, 2004. ISSN 1467-8659. doi:10.1111/j.1467-8659.2004.00753.x. URL <http://dx.doi.org/10.1111/j.1467-8659.2004.00753.x>.
- Frits H. Post, Benjamin Vrolijk, Helwig Hauser, Robert S. Laramee, and Helmut Doleisch. The State of the Art in Flow Visualisation: Feature Extraction and Tracking. *Computer Graphics Forum*, 2003. ISSN 1467-8659.

doi:10.1111/j.1467-8659.2003.00723.x.

- Tobias Günther and Holger Theisel. The state of the art in vortex extraction. *Computer Graphics Forum*, 2017.
- Armin Pobitzer, Ronald Peikert, Raphael Fuchs, Benjamin Schindler, Alexander Kuhn, Holger Theisel, Kresimir Matkovic, and Helwig Hauser. The State of the Art in Topology?Based Visualization of Unsteady Flow. *Computer Graphics Forum*, 2011a. ISSN 1467-8659. doi:org:443/handle/10.1111/v30i6pp1789-1811.
- T. Salzbrunn, H. Jänicke, T. Wischgoll, and Gerek Scheuermann. The state of the art in flow visualization: Partition-based techniques. In H. Hauser, S. Strassburger, and H. Theisel, editors, *Simulation and Visualization 2008*, pages 75–92. SCS Publishing House, SCS Publishing House, 2008.
- Andrea Brambilla, Robert Carnecky, Ronald Peikert, Ivan Viola, and Helwig Hauser. Illustrative Flow Visualization: State of the Art, Trends and Challenges. In Marie-Paule Cani and Fabio Ganovelli, editors, *Eurographics 2012 - State of the Art Reports*. The Eurographics Association, 2012. doi:10.2312/conf/EG2012/stars/075-094.
- James L. Helman and Lambertus Hesselink. Representation and display of vector field topology in fluid flow data sets. *IEEE Computer*, 22(8):27–36, 1989.
- Gerek Scheuermann, Heinz Krüger, Martin Menzel, and Alyn P. Rockwood. Visualizing non-linear vector field topology. *IEEE Transactions on Visualization and Computer Graphics*, 4(2):109–116, 1998.
- Wim de Leeuw and Robert van Liere. Collapsing flow topology using area metrics. In *Proc. IEEE Visualization '99*, pages 149–354, 1999a.
- Thomas Wischgoll and Gerek Scheuermann. Detection and visualization of closed streamlines in planar flows. *IEEE Transactions on Visualization and Computer Graphics*, 7(2):165–172, 2001.
- Wim de Leeuw and Robert van Liere. Visualization of global flow structures using multiple levels of topology. In *Data Visualization 1999. Proc. VisSym 99*, pages 45–52, 1999b.
- Xavier Tricoche, Gerek Scheuermann, and Hans Hagen. A topology simplification method for 2D vector fields. In *Proc. IEEE Visualization*, pages 359–366, 2000.
- Xavier Tricoche, Gerek Scheuermann, and Hans Hagen. Continuous topology simplification of planar vector fields. In *Proc. IEEE Visualization*, pages 159 – 166, 2001.
- Rüdiger Westermann, Christopher Johnson, and Thomas Ertl. Topology-preserving smoothing of vector fields. *IEEE Transactions on Visualization and Computer Graphics*, 7(3):222–229, 2001.
- Suresh K. Lodha, Jose C. Renteria, and Krishna M. Roskin. Topology preserving compression of 2D vector fields. In *Proc. IEEE Visualization*, pages 343–350, 2000.
- Nikolai M. Faaland Suresh Lodha and Jose C. Renteria. Topology preserving top-down compression of 2D vector fields using bintree and triangular quadtrees. *IEEE Transactions on Visualization and Computer Graphics*, 9(4):433–442, 2003.
- Holger Theisel, Christian Rössl, and Hans-Peter Seidel. Compression of 2D vector fields under guaranteed topology preservation. *Computer Graphics Forum (Eurographics 2003)*, 22(3):333–342, 2003a.
- Holger Theisel. Designing 2D vector fields of arbitrary topology. *Computer Graphics Forum (Eurographics 2002)*, 21(3):595–604, 2002.
- Tino Weinkauff, Holger Theisel, Hans-Christian Hege, and Hans-Peter Seidel. Topological construction and visualization of higher order 3D vector fields. *Computer Graphics Forum (Proc. Eurographics)*, 23(3):469–478, 2004a.
- Al Globus, Creon Levit, and Tom A. Lasinski. A tool for visualizing the topology of three-dimensional vector fields. In *Proc. IEEE Visualization*, pages 33–40, 1991.
- James L. Helman and Lambertus Hesselink. Visualizing vector field topology in fluid flows. *IEEE Computer Graphics and Applications*, 11:36–46, 1991.
- Karim M. Mahrous, Janine C. Bennett, Bernd Hamann, and Kenneth I. Joy. Improving topological segmentation of three-dimensional vector fields. In *Data Visualization (Proc. VisSym)*, pages 203–212, 2003.
- Karim M. Mahrous, Janine C. Bennett, Gerek Scheuermann, Bernd Hamann, and Kenneth I. Joy. Topological segmentation in three-dimensional vector fields. *IEEE Transactions on Visualization and Computer Graphics*, 10(2): 198–205, 2004.
- Holger Theisel, Tino Weinkauff, Hans-Christian Hege, and Hans-Peter Seidel. Saddle connectors - an approach to visualizing the topological skeleton of complex 3D vector fields. In *Proc. IEEE Visualization 2003*, pages 225–232, 2003b.

- Tino Weinkauff, Holger Theisel, Hans-Christian Hege, and Hans-Peter Seidel. Boundary switch connectors for topological visualization of complex 3D vector fields. In *Data Visualization (Proc. VisSym)*, pages 183–192, 2004b.
- Robert S. Laramee, Helwig Hauser, Lingxiao Zhao, and Frits H. Post. Topology-based flow visualization, the state of the art. In Helwig Hauser, Hans Hagen, and Holger Theisel, editors, *Topology-based Methods in Visualization, Mathematics and Visualization*, pages 1–19. Springer, 2007. ISBN 978-3-540-70822-3. doi:10.1007/978-3-540-70823-0\_1. URL [http://dx.doi.org/10.1007/978-3-540-70823-0\\_1](http://dx.doi.org/10.1007/978-3-540-70823-0_1).
- Armin Pobitzer, Ronald Peikert, Raphael Fuchs, Benjamin Schindler, Alexander Kuhn, Holger Theisel, Kresimir Matkovic, and Helwig Hauser. The state of the art in topology-based visualization of unsteady flow. *Computer Graphics Forum*, 30(6):1789–1811, 2011b. ISSN 1467-8659.
- Wentao Wang, Wenke Wang, and Sikun Li. From numerics to combinatorics: a survey of topological methods for vector field visualization. *Journal of Visualization*, pages 1–26, 2016.
- Christian Heine, Heike Leitte, Mario Hlawitschka, Federico Iuricich, Leila De Floriani, Gerik Scheuermann, Hans Hagen, and Christoph Garth. A survey of topology-based methods in visualization. In *Computer Graphics Forum*, volume 35, pages 643–667. Wiley Online Library, 2016.
- George Haller. Distinguished material surfaces and coherent structures in three-dimensional fluid flows. *Physica D*, 149:248–277, 2001.
- George Haller and Guo-Cheng Yuan. Lagrangian coherent structures and mixing in two-dimensional turbulence. *Physica D*, 147(3-4):352–370, 2000. ISSN 0167-2789. doi:[http://dx.doi.org/10.1016/S0167-2789\(00\)00142-1](http://dx.doi.org/10.1016/S0167-2789(00)00142-1).
- Armin Pobitzer, Ronald Peikert, Raphael Fuchs, Holger Theisel, and Helwig Hauser. Filtering of FTLE for visualizing spatial separation in unsteady 3D flow. In *Topological Methods in Data Analysis and Visualization II*, pages 237–253. Springer, 2012.
- George Haller. Lagrangian coherent structures from approximate velocity data. *Physics of Fluids*, 14(6), 2002. doi:<http://dx.doi.org/10.1063/1.1477449>.
- Francois Lekien, Chad Coulliette, Arthur J. Mariano, Edward H. Ryan, Lynn K. Shay, George Haller, and Jerry Marsden. Pollution release tied to invariant manifolds: A case study for the coast of Florida. *Physica D*, 210(1):1–20, 2005.
- Shawn C. Shadden, Francois Lekien, Jeffrey D. Paduan, Francisco P. Chavez, and Jerrold E. Marsden. The correlation between surface drifters and coherent structures based on high-frequency radar data in Monterey Bay. *Deep Sea Research Part II: Topical Studies in Oceanography*, 56(3-5):161–172, 2009. ISSN 0967-0645. doi:DOI: 10.1016/j.dsr2.2008.08.008. URL <http://www.sciencedirect.com/science/article/B6VGC-4TJ1HH1-3/2/9f098e9e2684e5cd8f53e69ab3c59c26>.
- Matthew J. Weldon, Thomas M. Peacock, Gustaaf Jacobs, Moneer Helu, and George Haller. Experimental and numerical investigation of the kinematic theory of unsteady separation. *Journal of Fluid Mechanics*, 611, 2008. doi:10.1017/S0022112008002395.
- Shawn C. Shadden, Francois Lekien, and Jerrold E. Marsden. Definition and properties of Lagrangian coherent structures from finite-time Lyapunov exponents in two-dimensional aperiodic flows. *Physica D*, 212(7):271–304, 2005. ISSN 0167-2789. doi:[http://dx.doi.org/10.1016/S0167-2789\(00\)00199-8](http://dx.doi.org/10.1016/S0167-2789(00)00199-8).
- Filip Sadlo and Daniel Weiskopf. Time-Dependent 2D Vector Field Topology: An Approach Inspired by Lagrangian Coherent Structures. *Computer Graphics Forum*, 29(1):88–100, 2010.
- Markus Uffinger, Filip Sadlo, and Thomas Ertl. A time-dependent vector field topology based on streak surfaces. *IEEE Transactions on Visualization and Computer Graphics*, 19(3):379–392, 2013.
- Doug Lipinski and Kamran Mohseni. A ridge tracking algorithm and error estimate for efficient computation of Lagrangian coherent structures. *Chaos: An Interdisciplinary Journal of Nonlinear Science*, 20(1):017504, 2010. doi:10.1063/1.3270049. URL <http://link.aip.org/link/?CHA/20/017504/1>.
- Tobias Günther, Alexander Kuhn, and Holger Theisel. MCFTLE: Monte Carlo rendering of finite-time Lyapunov exponent fields. *Computer Graphics Forum (Proc. EuroVis)*, 35(3):381–390, 2016.
- Christoph Garth, Xavier Tricoche Guo-Shi Li, Charles D. Hansen, and Hans Hagen. Visualization of coherent structures in transient 2D flows. In *Proceedings of TopoInVis 2007*, pages 1–13, 2009.
- Christoph Garth, Florian Gerhardt, Xavier Tricoche, and Hans Hagen. Efficient computation and visualization of coherent structures in fluid flow applications. *IEEE Transactions on Visualization and Computer Graphics*, 13(6): 1464–1471, 2007. ISSN 1077-2626. doi:<http://doi.ieeecomputersociety.org/10.1109/TVCG.2007.70551>.
- Filip Sadlo and Ronald Peikert. Visualizing Lagrangian coherent structures and comparison to vector field topology. In *Proceedings of TopoInVis 2007*, pages 15–30, 2009.

- Filip Sadlo and Ronald Peikert. Efficient visualization of Lagrangian coherent structures by filtered AMR ridge extraction. *IEEE Transactions on Visualization and Computer Graphics (Proceedings Visualization)*, 13(6):1456–1463, 2007.
- Filip Sadlo, Alessandro Rigazzi, and Ronald Peikert. Time-Dependent Visualization of Lagrangian Coherent Structures by Grid Advection. In *Proceedings of TopoInVis 2009*, pages 151–165. Springer, 2011.
- Harsh Bhatia, Valerio Pascucci, Robert M. Kirby, and Peer-Timo Bremer. Extracting features from time-dependent vector fields using internal reference frames. *Computer Graphics Forum (Proc. EuroVis)*, 33(3):21–30, June 2014.
- Alexander Wiebel, Christoph Garth, and Gerek Scheuermann. Computation of localized flow for steady and unsteady vector fields and its applications. *IEEE Transactions on Visualization and Computer Graphics*, 13(4):641–651, 2007.
- Roxana Bujack, Mario Hlawitschka, and Kenneth I Joy. Topology-inspired galilean invariant vector field analysis. In *2016 IEEE Pacific Visualization Symposium (PacificVis)*, pages 72–79. IEEE, 2016.
- Robin Forman. A user’s guide to discrete morse theory. In *Proc. of the 2001 Internat. Conf. on Formal Power Series and Algebraic Combinatorics, A special volume of Advances in Applied Mathematics*, page 48, 2001.
- Jan Reininghaus and Ingrid Hotz. Combinatorial 2d vector field topology extraction and simplification. In Valerio Pascucci, Xavier Tricoche, Hans Hagen, and Julien Tierny, editors, *Topological Methods in Data Analysis and Visualization*, pages 103 – 114. 2011. ISBN 978-3-642-15013-5. doi:10.1007/978-3-642-15014-2\_9.
- K. Mischaikow, E. Zhang, P. Pilarczyk, G. Chen, and R. S. Laramée. Vector field editing and periodic orbit extraction using morse decomposition. *IEEE Transactions on Visualization & Computer Graphics*, 13:769–785, 07 2007. ISSN 1077-2626. doi:10.1109/TVCG.2007.1021. URL doi.ieeecomputersociety.org/10.1109/TVCG.2007.1021.
- Harsh Bhatia, Shreeraj Jadhav, Peer-Timo Bremer, Guoning Chen, Joshua A. Levine, Luis Gustavo Nonato, and Valerio Pascucci. Flow visualization with quantified spatial and temporal errors using edge maps. *IEEE Trans. Vis. Comput. Graph.*, 18(9):1383–1396, 2012. doi:10.1109/TVCG.2011.265. URL <https://doi.org/10.1109/TVCG.2011.265>.
- Primoz Skraba, Paul Rosen, Bei Wang, Guoning Chen, Harsh Bhatia, and Valerio Pascucci. Critical point cancellation in 3d vector fields: Robustness and discussion. *Transactions on Visualization and Computer Graphics*, 2016.
- Bei Wang, Paul Rosen, Primoz Skraba, Harsh Bhatia, and Valerio Pascucci. Visualizing robustness of critical points for 2d time-varying vector fields. *Comput. Graph. Forum*, 32(3):221–230, 2013. doi:10.1111/cgf.12109. URL <https://doi.org/10.1111/cgf.12109>.
- Herbert Edelsbrunner, John Harer, and Afra Zomorodian. Hierarchical morse complexes for piecewise linear 2-manifolds. In *Proceedings of the Seventeenth Annual Symposium on Computational Geometry, SCG ’01*, pages 70–79, New York, NY, USA, 2001. ACM. ISBN 1-58113-357-X. doi:10.1145/378583.378626. URL <http://doi.acm.org/10.1145/378583.378626>.
- Peer-Timo Bremer, Herbert Edelsbrunner, Bernd Hamann, and Valerio Pascucci. A topological hierarchy for functions on triangulated surfaces. *IEEE Trans. Vis. Comput. Graph.*, 10(4):385–396, 2004. doi:10.1109/TVCG.2004.3. URL <https://doi.org/10.1109/TVCG.2004.3>.
- Herbert Edelsbrunner, John Harer, Vijay Natarajan, and Valerio Pascucci. Morse-smale complexes for piecewise linear 3-manifolds. In *Proceedings of the 19th ACM Symposium on Computational Geometry, San Diego, CA, USA, June 8-10, 2003*, pages 361–370, 2003. doi:10.1145/777792.777846. URL <http://doi.acm.org/10.1145/777792.777846>.
- Attila Gyulassy, Vijay Natarajan, Valerio Pascucci, Peer-Timo Bremer, and Bernd Hamann. Topology-based simplification for feature extraction from 3d scalar fields. In *16th IEEE Visualization Conference, VIS 2005, Minneapolis, MN, USA, October 23-28, 2005*, pages 535–542, 2005. doi:10.1109/VISUAL.2005.1532839. URL <https://doi.org/10.1109/VISUAL.2005.1532839>.
- Thomas Lewiner, Hélio Lopes, and Geovan Tavares. Applications of forman’s discrete morse theory to topology visualization and mesh compression. *IEEE Trans. Vis. Comput. Graph.*, 10(5):499–508, 2004. doi:10.1109/TVCG.2004.18. URL <https://doi.org/10.1109/TVCG.2004.18>.
- Attila Gyulassy, Harsh Bhatia, Peer-Timo Bremer, and Valerio Pascucci. Computing accurate morse-smale complexes from gradient vector fields. In *Green in Software Engineering*, pages 205–218. 2015. doi:10.1007/978-3-662-44900-4\_12. URL [https://doi.org/10.1007/978-3-662-44900-4\\_12](https://doi.org/10.1007/978-3-662-44900-4_12).
- Attila Gyulassy, Vijay Natarajan, Valerio Pascucci, and Bernd Hamann. Efficient computation of morse-smale complexes for three-dimensional scalar functions. *IEEE Trans. Vis. Comput. Graph.*, 13(6):1440–1447, 2007. doi:10.1109/TVCG.2007.70552. URL <https://doi.org/10.1109/TVCG.2007.70552>.

- Paolo Cignoni, D. Constanza, Claudio Montani, Claudio Rocchini, and Roberto Scopigno. Simplification of tetrahedral meshes with accurate error evaluation. In *IEEE Visualization 2000, October 8-13, 2000, Hilton Hotel, Salt Lake City, Utah, USA, Proceedings.*, pages 85–92, 2000. doi:10.1109/VISUAL.2000.885680. URL <https://doi.org/10.1109/VISUAL.2000.885680>.
- Hamish Carr, Jack Snoeyink, and Michiel van de Panne. Simplifying flexible isosurfaces using local geometric measures. In *15th IEEE Visualization 2004 Conference, VIS 2004, Austin, TX, USA, October 10-15, 2004*, pages 497–504, 2004. doi:10.1109/VISUAL.2004.96. URL <https://doi.org/10.1109/VISUAL.2004.96>.
- Igor Guskov and Zoë J. Wood. Topological noise removal. In *Proceedings of the Graphics Interface 2001 Conference, Ottawa, Ontario, Canada, June 7-9, 2001*, pages 19–26, 2001. URL <http://www.graphicsinterface.org/proceedings/2001/121/>.
- Shigeo Takahashi, Gregory M. Nielson, Yuriko Takeshima, and Issei Fujishiro. Topological volume skeletonization using adaptive tetrahedralization. In *2004 Geometric Modeling and Processing (GMP 2004), Theory and Applications, 13-15 April 2004, Beijing, China*, pages 227–236, 2004. doi:10.1109/GMAP.2004.1290044. URL <https://doi.org/10.1109/GMAP.2004.1290044>.
- Hamish Carr, Jack Snoeyink, and Ulrike Axen. Computing contour trees in all dimensions. *Comput. Geom.*, 24(2):75–94, 2003. doi:10.1016/S0925-7721(02)00093-7. URL [https://doi.org/10.1016/S0925-7721\(02\)00093-7](https://doi.org/10.1016/S0925-7721(02)00093-7).
- Julien Tierny, Joel Daniels II, Luis Gustavo Nonato, Valerio Pascucci, and Cláudio T. Silva. Interactive quadrangulation with reeb atlases and connectivity textures. *IEEE Trans. Vis. Comput. Graph.*, 18(10):1650–1663, 2012. doi:10.1109/TVCG.2011.270. URL <https://doi.org/10.1109/TVCG.2011.270>.
- A. Clebsch. Ueber die integration der hydrodynamischen gleichungen. *Journal für die reine und angewandte Mathematik*, 56:1–10, 1859. URL <http://eudml.org/doc/147740>.
- Peter Kotiuga. Clebsch potentials and the visualization of three-dimensional solenoidal vector fields. 27:3986 – 3989, 10 1991.
- Jinhee Jeong and Fazle Hussain. On the identification of a vortex. *Journal of Fluid Mechanics*, 285:69–94, 1995. doi:10.1017/S0022112095000462.
- Axel Brandenburg. Magnetic field evolution in simulations with euler potentials. *Monthly Notices of the Royal Astronomical Society*, 401(1):347–354, 2010. ISSN 1365-2966. doi:10.1111/j.1365-2966.2009.15640.x. URL <http://dx.doi.org/10.1111/j.1365-2966.2009.15640.x>.
- Pengyu He and Yue Yang. Construction of initial vortex-surface fields and clebsch potentials for flows with high-symmetry using first integrals. *Physics of Fluids*, 28(3):037101, 2016. doi:10.1063/1.4943368.
- C. Robin Graham and Frank S. Henyey. Clebsch representation near points where the vorticity vanishes. *Physics of Fluids*, 12(4):744–746, 2000. doi:10.1063/1.870331.
- Albert Chern, Felix Knöppel, Ulrich Pinkall, and Peter Schröder. Inside fluids: Clebsch maps for visualization and processing. *ACM Trans. Graph.*, 36(4):142:1–142:11, July 2017. doi:10.1145/3072959.3073591. URL <http://dx.doi.org/10.1145/3072959.3073591>.
- Alexis Angelidis and Karan Singh. Kinodynamic skinning using volume-preserving deformations. In *Proceedings of the 2007 ACM SIGGRAPH/Eurographics Symposium on Computer Animation, SCA '07*, pages 129–140, Aire-la-Ville, Switzerland, Switzerland, 2007. Eurographics Association. ISBN 978-1-59593-624-0. URL <http://dl.acm.org/citation.cfm?id=1272690.1272709>.
- Wolfram von Funck, Holger Theisel, and Hans-Peter Seidel. Vector field based shape deformations. *ACM Trans. Graph.*, 25(3):1118–1125, July 2006. ISSN 0730-0301. doi:10.1145/1141911.1142002. URL <http://doi.acm.org/10.1145/1141911.1142002>.
- G Zigelman, Ron Kimmel, and Nahum Kiryati. Texture mapping using surface flattening via multidimensional scaling. 8:198–207, 05 2002.
- Kai Hormann, Konrad Polthier, and Alla Sheffer. Mesh parameterization: Theory and practice. In *ACM SIGGRAPH ASIA 2008 Courses, SIGGRAPH Asia '08*, pages 12:1–12:87, New York, NY, USA, 2008. ACM. doi:10.1145/1508044.1508091. URL <http://doi.acm.org/10.1145/1508044.1508091>.
- Hans-Christian Ebke, Patrick Schmidt, Marcel Campen, and Leif Kobbelt. Interactively controlled quad remeshing of high resolution 3d models. *ACM Trans. Graph.*, 35(6):218:1–218:13, November 2016. ISSN 0730-0301. doi:10.1145/2980179.2982413. URL <http://doi.acm.org/10.1145/2980179.2982413>.
- M. Campen and L. Kobbelt. Quad Layout Embedding via Aligned Parameterization. *Computer Graphics Forum*, 2014. ISSN 1467-8659. doi:10.1111/cgf.12401.

- Jeff Erickson and Sarel Har-Peled. Optimally cutting a surface into a disk. In *Proceedings of the Eighteenth Annual Symposium on Computational Geometry*, SCG '02, pages 244–253, New York, NY, USA, 2002. ACM. ISBN 1-58113-504-1. doi:10.1145/513400.513430. URL <http://doi.acm.org/10.1145/513400.513430>.
- A. Friederici, C. Rössl, and H. Theisel. Finite time steady 2d vector field topology. In *Topological Methods in Data Analysis and Visualization IV*, pages 253–266, 2017.
- H. Theisel, T. Weinkauff, H.-C. Hege, and H.-P. Seidel. Grid-independent detection of closed stream lines in 2d vector fields. In *Proc. Vision, Modeling and Visualization (VMV) 2004*, pages 421–428, Stanford, USA, November 15–18 2004.
- T. Weinkauff, H. Theisel, H.-C. Hege, and H.-P. Seidel. *Boundary Switch Connectors for Topological Visualization of Complex 3D Vector Fields*, pages 183–192. 2004c.